First-principles study of the Fe|MgO(0 0 1) interface: magnetic anisotropy

Thomas Bose[1,3]**, Ramon Cuadrado**[1,4]**, Richard F L Evans**[1]**, Roman V Chepulskii**[2]**, Dmytro Apalkov**[2] **and Roy W Chantrell**[1]

[1] Department of Physics, University of York, Heslington, York YO10 5DD, UK
[2] Samsung Electronics, Semiconductor R&D Center (Grandis), San Jose, CA 95134, USA

E-mail: t.bose@sheffield.ac.uk

CrossMark

Abstract

We present a systematic first-principles study of Fe|MgO bilayer systems emphasizing the influence of the iron layer thickness on the geometry, the electronic structure and the magnetic properties. Our calculations ensure the unconstrained structural relaxation at scalar relativistic level for various numbers of iron layers placed on the magnesium oxide substrate. Our results show that due to the formation of the interface the electronic structure of the interface iron atoms is significantly modified involving charge transfer within the iron subsystem. In addition, we find that the magnetic anisotropy energy increases from 1.9 mJ m^{-2} for 3 Fe layers up to 3.0 mJ m^{-2} for 11 Fe layers.

Keywords: magnetism, magnetic anisotropy, density functional theory, electronic structure

(Some figures may appear in colour only in the online journal)

1. Introduction

Enhancing the prospect of high density magnetic data storage devices reaching market maturity requires comprehensive studies including the identification of both appropriate materials and optimized geometrical configurations. During the last decade much progress has been made in magnetic materials science to cull promising candidates from the pool of possible materials and their geometrical arrangement based on experimental [1–7] and computational [8–14] studies. Materials bearing the high potential to find application in future magnetic recording media and magnetoresistive random access memory (MRAM) devices need to exhibit a large magnetocrystalline anisotropy energy (MAE) [15].

In this regard, magnetic tunnel junctions (MTJs), for example, are under intense investigation. Material combinations such as CoFeB|MgO [7, 16–18], FeCo|MgO|FeCo [8, 19–21], CoPt|MgO|CoPt [22] or junctions containing Fe|MgO interfaces [23–27] are thought to play an important role in future data storage devices. Recently, conductance anomalies

of CoFeB|MgO|CoFeB MTJs were reported [28] and the role of boron diffusion in CoFe|MgO tunnel junctions was discussed [29]. Related to the search for promising material combinations, epitaxial Co$_{1.5}$Fe$_{1.5}$Ge(0 0 1) electrodes were recently tested in MgO-based MTJs using spin- and symmetry-resolved photoemission [30].

The present study analyzes Fe|MgO bilayer systems and thus complements previous studies on this transition metal|insulator interface. The importance of the interface in Fe|MgO bilayer systems related to Fe–O electron hybridization was shown in [31] and recently underpinned in [32] where magnetic properties of individual Fe atoms deposited on MgO(1 0 0) thin films were studied. The sensitivity to interface conditions of these kinds of material combinations was further demonstrated by showing the influence of an electric field on magnetic anisotropy and magnetisation [3, 25, 33–36]. Moreover, transport properties influenced by structural defects were investigated in [37]. In this work the authors observed an enhanced magnetoresistance due to monoatomic roughness in epitaxial Fe|MgO|Fe systems. Further to this, it was shown that the antiferromagnetic interlayer exchange coupling in Fe|MgO|Fe tunnel junctions is affected by the oxygen concentration at the Fe|MgO interface [24]. It is also known that electronic transport is extremely sensitive to the

[3] Present address: Department of Computer Science, University of Sheffield, Regent Court, Sheffield S1 4DP, UK.
[4] Present address: Institut Català de Nanociència i Nanotecnologia, Campus de la UAB, Edifici ICN2, 08193 Bellaterra, Barcelona, Spain.

method used to relax the structure, i.e. using local spin-density approximation or generalized gradient approximation (GGA) [23]. In our calculations we employ the GGA method and observe sensitivity of the transference of the electric charge depending on the iron thickness. Previously, it was reported in [16, 27, 31] that changing the thickness of magnesium oxide affects the magnetic anisotropy only slightly, whereas the iron thickness influences the MAE significantly. This was underlined by an onsite projected analysis for the magnetic anisotropy [27]. In the present paper we therefore focus on the magnetic properties of the Fe|MgO interface in dependence on the iron layer thickness. More precisely, we have undertaken calculations of electronic structure and magnetic anisotropy energies by means of density functional theory (DFT) using a fully relativistic implementation [38] in the GREEN [39] code employing the SIESTA [40] framework. In particular, we show the effect of varying iron thickness on these quantities taking into account unconstrained structural relaxation of the overall Fe|MgO bilayer system. We find MAE values up to 3.0 mJ m^{-2} which is in agreement with the values reported in [31].

The paper is structured as follows: in section 2 the theoretical methods employed in the calculations are explained and the main density functional parameters are given. The relaxation analysis and electronic survey of each geometric configuration are described in sections 3.1 and 3.2. A layer resolved study of the magnetic moments is presented in section 3.3. Subsequent, the effect of the lattice parameters and the number of Fe layers on the magnetic anisotropy is analised and interpreted in section 3.4. Finally, the conclusion is given in section 4.

2. Model and computational method

By means of DFT we investigated the geometric, electronic and magnetic properties of Fe|MgO(0 0 1) interfaces. Based on previous theoretical studies, we have located the interfacial Fe atoms directly above the oxygen atoms due to the significantly lower energy of this configuration [12, 13]. The corresponding Fe|MgO interfacial structure and the Fe as well as MgO unit cells are depicted in figure 1. Performing a systematic size-dependent study, we have modeled 5 different systems composed of $n_{Fe} = 3, 5, 7, 9$ and 11 Fe plus 5MgO planes. These n_{Fe}Fe|5MgO-structures were repeated in the out-of-plane direction.

We have optimized each one of the geometric configurations under the conjugate gradient (CG) approximation without any constraint. The relaxations have been performed at the scalar relativistic level until the forces between atoms were less than 0.03 eV Å^{-1}. In all cases the initial common in-plane lattice vector to perform the calculations was the bulk MgO optimized value a_{MgO} due to its greater structural rigidity compared to Fe. During the relaxation process the in-plane and out-of-plane values were allowed to change. We discuss this aspect in the next section (see figure 2). As exchange correlation (XC) potential we employed the GGA using the

Perdew, Burke, and Ernzerhof parametrization [41]. The basis set comprises double-ζ polarized strictly localized numerical atomic orbitals. For the optimization process we used up to 800 k points in the Brillouin zone. Real-space integrals were computed over a three-dimensional grid with a resolution of 700 Ry. The magnetic properties, however, are quite sensitive to these parameters. Hence we increased the number of k-points up to 9000 and the grid resolution in real space up to 1800 Ry. We have checked the convergence of results with respect to the number of k-points and grid resolution. The energy tolerance between two selfconsistent (SC) energy steps was set to $E_{tol}^{SC} \leqslant 10^{-4}$ eV. The parameters mentioned above provide a reasonable trade-off between accuracy and computation time.

3. Results and discussion

3.1. Relaxation

In what follows we present the results of the relaxation process of the n_{Fe}Fe|5MgO configurations for $n_{Fe} = 3, 5, 7, 9$ and 11. We find that the favoured final configuration of the system is *body centred tetragonal* (*bct*) Fe|MgO. We obtain the Fe-thickness dependent evolution of the in-plane lattice parameter *a* and its out-of-plane *c/a* counterpart as shown in figure 2. Starting from the optimized bulk MgO lattice constant a_{MgO} as initial guess for the Fe|MgO lattice parameter we observe a small decrease of the in-plane lattice parameter (denoted *a*) when $n_{Fe} = 3$, which is almost the same as its initial guess and is around 3.05 Å. Increasing the number of iron layers we observe a decrease of the in-plane value down to 3.0 Å for $n_{Fe} = 9$. The largest system under study ($n_{Fe} = 11$) exhibits no further significant change of the in-plane lattice parameter compared with $n_{Fe} = 9$.

Inspecting figure 2 clearly shows that MgO plays an important role in the metastable geometries because the optimized *a*-value only deviates about 1.5% with respect to the MgO bulk value. However, the c/a ratio between Fe planes changes in bigger percentage with Fe thickness from 0.820 up to 0.895 which corresponds to a variation of around 0.19 Å. Given that the c-value increases simultaneously with the decrease of the in-plane lattice constant (roughly preserving the volume per Fe atom), the different behaviour between the thickness-dependence of *a* and the *c/a*-ratio is reasonable. The general trend that the value of the in-plane lattice constant changes towards the bulk-Fe value when adding more iron layers demonstrates that the influence of the MgO-substrate becomes less dominant for thicker iron systems. As the Fe and MgO planes have different numbers of atoms, the MgO is denser than the Fe. For a small number of Fe planes the Fe atoms are therefore more likely to adapt to the MgO lattice constant. Hence, the Fe planes tend to be closer than the MgO ones. However, this changes when increasing the number of Fe planes. In particular, this emphasizes the importance of Fe|MgO-interfaces regarding the structural characterization of functional devices employing ultrathin magnetic iron films grown on the substrate MgO.
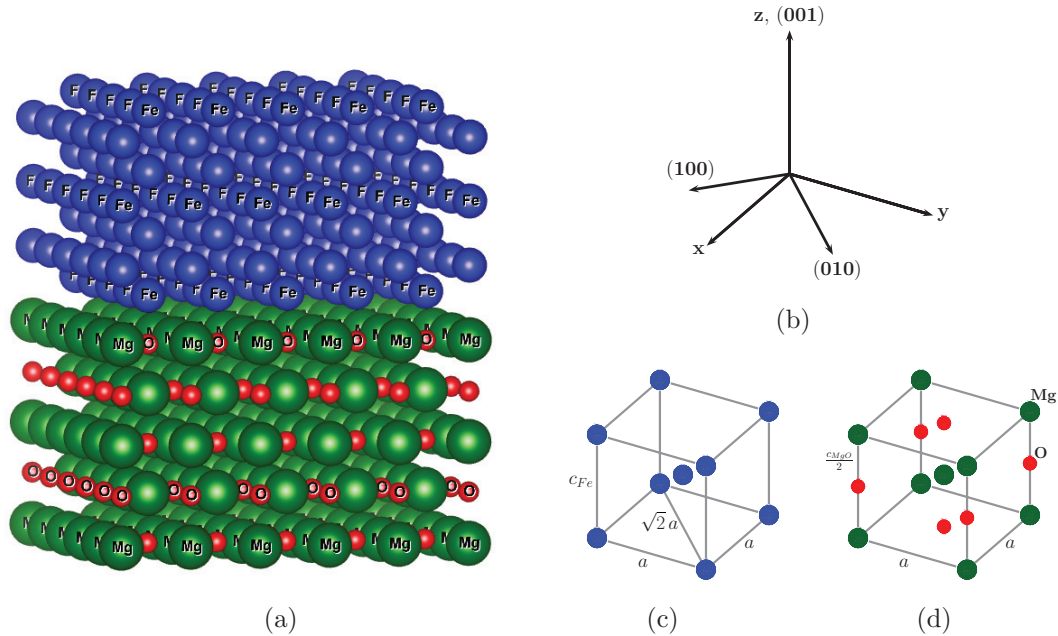
Figure 1. Geometry and structure of the Fe|MgO systems. In (a) the slab geometry is shown for 7 Fe on 5 MgO layers. The coordinate system in (b) corresponds to the Fe and MgO unit cells in (c) and (d).
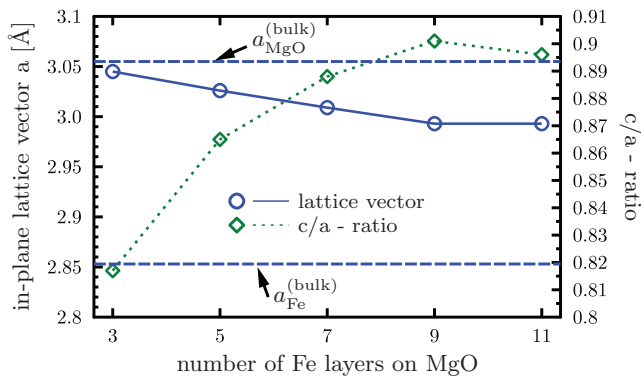
Figure 2. In-plane (*a*, blue circles) and out-of-plane (*c/a*, green diamonds) lattice constants as a function of the number of iron layer slice. The *c*-values are averaged over all Fe planes. The lines are guides to the eye. Fe and MgO bulk $a_{\mathrm{Fe,MgO}}$ values are presented with blue dashed lines.

To discuss the out-of-plane distances in more detail we refer to table 1. Here, we compare the Fe–O, Fe–Fe and Mg–O distances from the interface up to the fourth Fe|MgO plane with the existing literature. We observe a good overall agreement. The main differences between our values and the ones reported in the literature arise at the interface. However, if we consider planes further away from the interface the deviations become smaller. It is worth mentioning that even though the XC functional used to perform the calculations is the same (GGA) and the interface configuration is similar, the small discrepancies in the distances could be due to the different number of the Fe planes, the kind of basis used (SIESTA works with localized atomic orbitals and VASP uses plane waves) and other DFT parameters specific to each code.

3.2. Density of states

Figure 3 shows the spin-up/-down projected density of states (PDOS) for the interfacial Fe and the next five Fe layers for the Fe configuration with $n_{\mathrm{Fe}} = 11$. Substantial changes appear in the interfacial Fe PDOS compared with the other PDOS-curves as well as the bulk density of states. As we have shown in the geometric characterization in section 3.1, the atoms at the interface are quite sensitive to the broken symmetry. From this observation one can expect non-conventional bulk effects in the electronic structure that cause changes in the magnetic moments and in the magnetic anisotropy of these bilayer systems. The up-/down-states are quite similar in all the Fe layers except the interface layer. The PDOS-curve representing the interface iron atom shows significant deviations in shape around the Fermi level compared to the other Fe layers. In particular, the peak just above the Fermi level for the down-states, not present in any other PDOS-plot, indicates the importance of the MgO substrate. Inspection of the Fe atoms located in Fe layers further away from the interface, a small peak at 0.25 eV can be observed. This peak, however, is much smaller than the one relating to the interface Fe atom and disappears in the bulk. Further to this, the Fe-*d* band is narrowed after putting Fe in contact with MgO.

To investigate the emergence of the peak shown by the interface Fe atoms we depict the interface Fe PDOS-curves for all system sizes analysed in our study in figure 4(a). It can clearly be seen that the peak in the spin-down band is located at 0.5 eV for $n_{\mathrm{Fe}} = 3$ and becomes more pronounced with increasing number of iron layers and, in addition, has moved closer to the Fermi level. There is also a peak in the spin-down states at about 2 eV which is presumably the residual of the peak in the bulk. To underline that this behaviour is

Table 1. Distances between neighbouring layers for the 11Fe|5MgO-system compared to values from the literature.

System	Method	$d_{-3}^{(z)}$ Mg(4)-O(3)	$d_{-2}^{(z)}$ O(3)-Mg(2)	$d_{-1}^{(z)}$ Mg(2)-O(1)	$d_0^{(z)}$ O(1)-Fe(1)	$d_1^{(z)}$ Fe(1)-Fe(2)	$d_2^{(z)}$ Fe(2)-Fe(3)	$d_3^{(z)}$ Fe(3)-Fe(4)
$[Fe]_{11}|[MgO]_5$	GGA[a] (SIESTA)	2.160	2.165	2.149	2.120	1.233	1.405	1.357
$[Fe]_{10}|[MgO]_6$	GGA[b] (VASP)	2.185	2.177	2.199	2.219	1.350	1.427	1.414
$[Fe_5(MgO)_5]_2$	GGA[c] (VASP)		2.111	2.094	2.092	1.231	1.392	

[a] Our study in this paper.
[b] Taken from [23].
[c] Taken from [24].

Note: We have adopted the notation $[Fe]_{11}|[MgO]_5$ for our system in this table to be better comparable to the systems studied in the references. The parameter $d_k^{(z)}$ represents a distance perpendicular to the film plane, the number k is only used to discriminate between the different distances. The number (i) in brackets behind the elements Mg, O and Fe denotes the plane number relative to the interface, i.e. $i = 1$ is the interface layer, $i = 2$ is the neighbouring layer and so on.
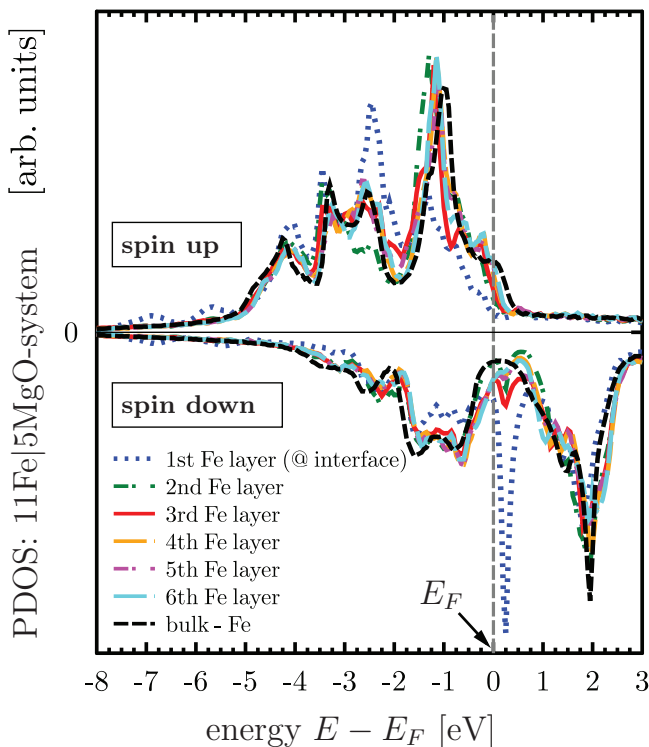
Figure 3. Fe spin-resolved density of states of the 11Fe|5MgO system projected on the first six Fe layers. *bcc*-Fe bulk density of states is also plotted in the figure (dashed black line).

unambiguously an interface effect we make the comparison with the PDOS of the second Fe layer. As is clear from figure 4(b), for $n_{Fe} = 3$ the peak just above E_f is located at 0.5 eV and is significantly reduced in height from its value in layer 1. As the Fe thickness increases, the position of the peak moves to the same energy value of 0.25 eV as in layer 1, again with significantly reduced peak value. Considering the spin-up PDOS-curves in both figures 4(a) and (b), the alterations in shape for different number of iron layers is less significant as compared to the spin-down curves. From this observation we conclude that the presence of the Fe|MgO interface has larger effect on the spin-down than on the spin-up electrons and hence creates impact on the magnetic structure.

Directly related with the electronic structure are the degree of tetragonality and the effect of the charge transferred between atoms, as illustrated in figures 5 and 6, respectively. As shown in section 3.1, the thicker the iron subsystem the more the in-plane lattice constant approaches the bulk-Fe value (Increasing the iron thickness decreases the in-plane lattice constant). From figure 4(a) it follows that the peak close to the Fermi energy in the spin-down curve becomes the more accentuated the more iron planes exist, that is if the degree of lattice distortion is lowered. Therefore, a change of tetragonality strongly affects the electronic structure of the interface Fe atoms. We performed additional calculations which support this finding. This means that we computed PDOS-curves relating to the 3Fe|5MgO system under variation of the in-plane lattice parameter (see figure 5). We also observe the formation of the peak in figure 5 which can be more clearly identified if tetragonality is reduced, i.e. if we go to smaller in-plane lattice parameters. However, it is less pronounced compared to the larger system sizes illustrated in figure 4(a). The graphical depiction of the charge transfer in figure 6 indicates that there is another effect involved to generate the peak in the spin-down density of states discussed above. First, the Fe-interface atoms need to have the possibility to donate a minimum amount of charge. This becomes clear from the drop of the total charge of the Fe layer located at the interface when changing $n_{Fe} = 3$ to $n_{Fe} = 5$. A comparison with figure 4(a) (see spin-down curves for $n_{Fe} = 3$ and $n_{Fe} = 5$) reveals that the peak evolves when the drop of the total charge occurs. Second, only a small amount of charge donated by the Fe-interface atom is transferred to the oxygen. The larger amount of charge remains in the iron film. Hence, a minimum number of iron layers seems to be required such that electrons originally belonging to the Fe-interface atoms can be distributed over several iron layers. To summarize, the presence and accentuation of the peak in figure 4(a) is due to tetragonality change and the donation of electric charge of the interface iron atoms within the total iron subsystem.

3.3. Magnetic moments

One of the most relevant physical properties that will change when the Fe atoms feel different environments is the magnetic moment (MM). We derived the MM values by subtracting the spin-down from the spin-up charge, having a MM enhancement when an excess of up charge arises. We calculated the
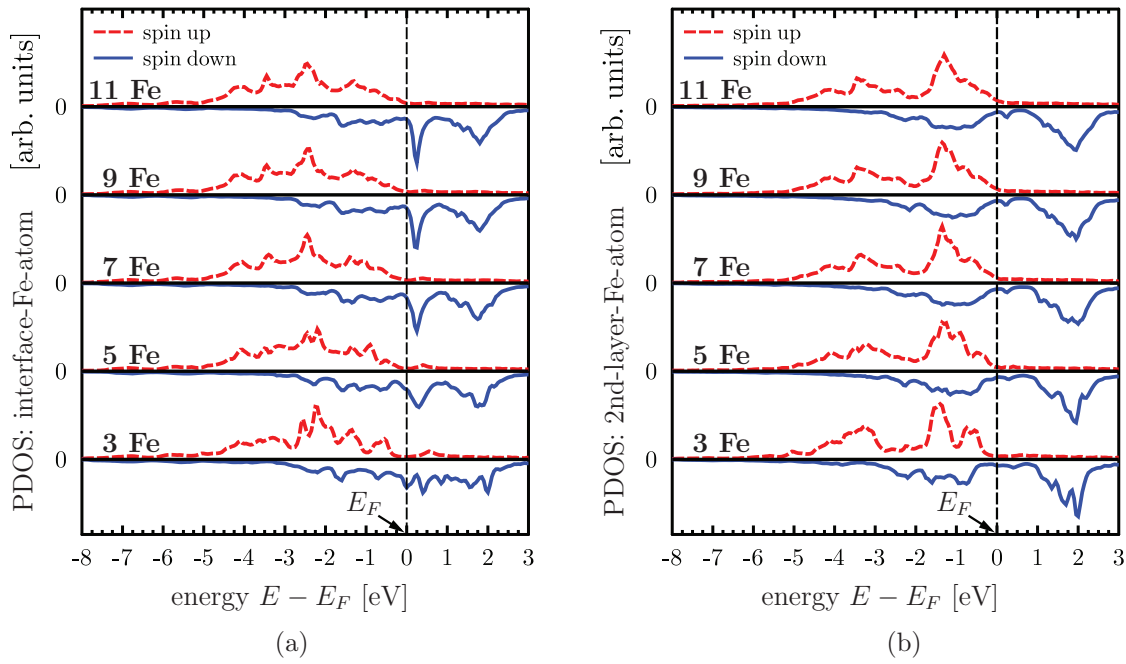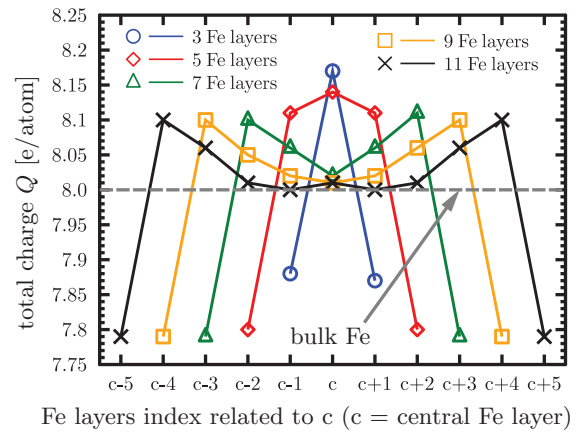
Figure 4. (a) Density of states projected on the Fe atom located at the interface depending on number of iron layers. (b) Density of states projected on Fe atom in second iron layer depending on number of iron layers.
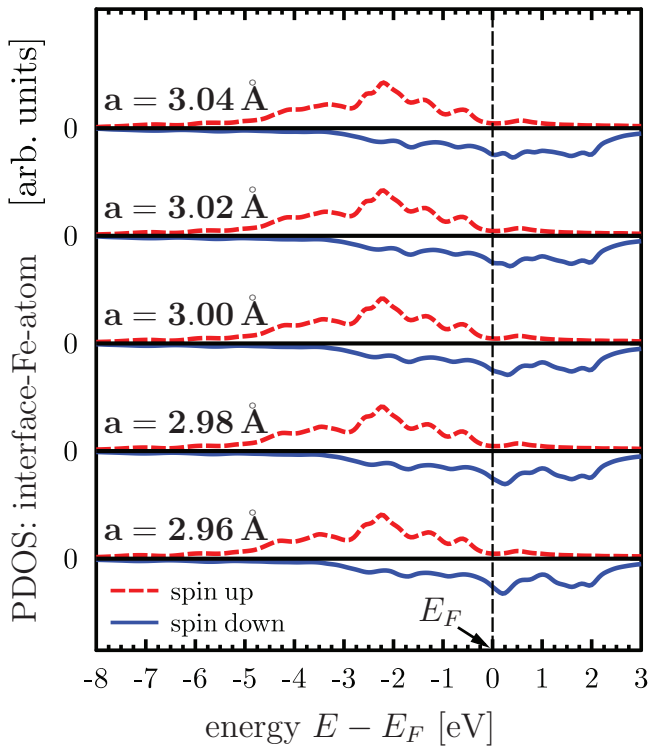

Figure 5. Density of states of the 3Fe|5MgO system projected on the Fe atom located at the interface for different in-plane lattice constants.

Figure 6. Net charge for different Fe thicknesses compared to the bulk Fe value of 8 e/atom. The values have been shifted to the centre of the Fe slice. The lines are guides for the eye.

spin-resolved charges using the Mulliken population analysis [42]. Figure 7(a) depicts the layer resolved iron MM per atom for all geometries studied in this work. We find that the interface Fe atoms possess the highest MM values. If we move from the interface towards the centre of the Fe film the MM values decrease. However, the values of the central magnetic moments are still significantly larger than the Fe bulk MM, even though

the values are reduced substantially compared with those at the interfaces. We also note that for the smallest configuration the dispersion in the MM values (MM-maximum minus MM-minimum) is only 0.14 μ_B/at increasing for the other configurations up to $\sim$0.6μ_B/at. In addition, we observe that the average MM value of the Fe atoms in the central iron plane decreases with increase of the number of iron layers. This is not surprising as a sufficient increase of iron planes should eventually resemble Fe bulk behaviour. Here, we observe this trend causing the magnetic moments to get closer to the bulk value, particularly in the centre of the slab. In figure 7(b) we have plotted the Fe interfacial MM values for all configurations with the aim to underline how the MM evolves as the number of Fe planes increases between the MgO material. There is a clear tendency to increase the MM for the bigger sizes. The difference between the MM values for $n_{Fe} = 3$ and

(a)

(b)
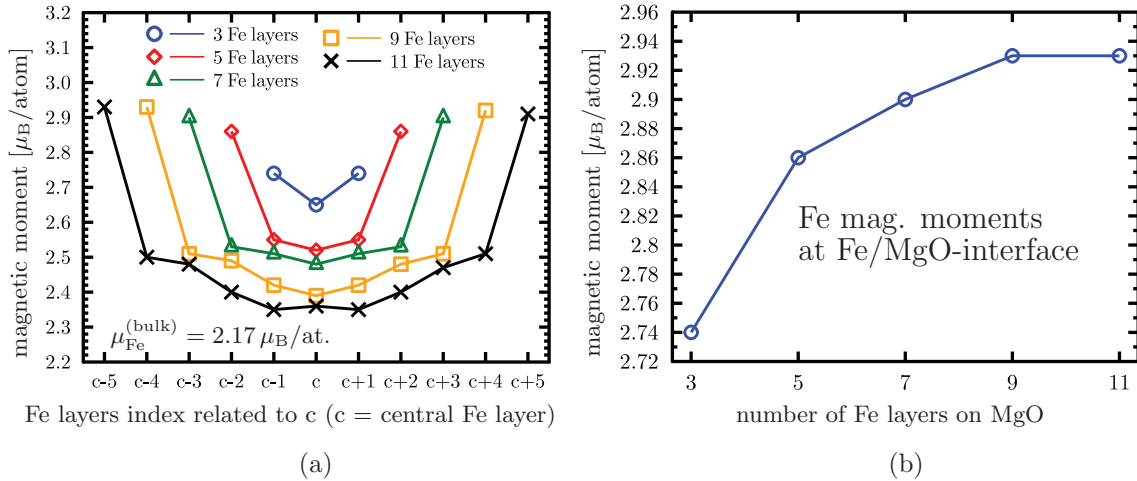
Figure 7. (a) Layer resolved magnetic moment of iron atoms for all configurations. The values have been shifted to the centre of the Fe slice. The lines are guides for the eye. (b) Interface Fe magnetic moment for different Fe thicknesses n_{Fe}. The solid line represents a guide for the eye. For comparison: the bulk-magnetic moment of iron is $\mu_{Fe}^{(bulk)} = 2.17\,\mu_B$/atom.

$n_{Fe} = 11$ is about 0.2 μ_B/at. This behavior is a consequence of the depopulation of up-states against the down ones, leading to an enhancement of the net MM of the interface Fe atoms.

3.4. Magnetocrystalline anisotropy energy

The magnetocrystalline anisotropy energy in dependence on the number of iron layers is presented in figure 8. The absolute value, obtained as the total energy difference between hard and easy quantization axis, has been divided by the area A_{Fe} (given by the square of the in-plane lattice constant) and by the volume V_{Fe} (representing the total volume of the iron subsystem). Firstly, we infer from the figure that the MAE/A_{Fe} increases from 1.9 mJ m^{-2} ($n_{Fe} = 3$) up to 3.0 mJ m^{-2} ($n_{Fe} = 11$). Layer-resolved MAE calculations are beyond the scope of the current work, however, this representation is most sensitive to the interface layer and suggests that the interfacial MAE increases with n_{Fe}. Secondly, the depicted behavior indicates that the MAE is likely to reach a plateau at some point when exceeding 11 Fe layers, that is if $n_{Fe} \gtrsim 11$. This is underpinned by the absolute value of the energy difference $|MAE(n_{Fe} = 11) - MAE(n_{Fe} = 9)| = 0.08$ meV, as obtained from the computation. Previous results indicate that the plateau is a maximum so that the MAE will decrease again when further increasing the Fe thickness [43, 44]. Dividing the absolute MAE value by the volume we clearly observe that the MAE/V_{Fe} decreases for increasing iron thickness. The explanation is that the largest contribution to the total anisotropy for these kinds of systems arises mainly from the interface, having almost constant contributions from the centre of the Fe layer. Therefore, for a large number of iron layers, i.e. $n_{Fe} \gg 11$, we expect that the MAE/$V_{Fe} \to 0$. In addition, the alteration of the c/a ratio for each configuration influences the magnetic anisotropy values, as other work demonstrates [12]. Hence, our calculated data emphasizes that the MAE is clearly an interface fact. However, it is not only the interface Fe layer that contributes to the MAE. Therefore, it is important to analyze the contributions of the first few iron layers next to the interface Fe layer within a layer-resolved study.
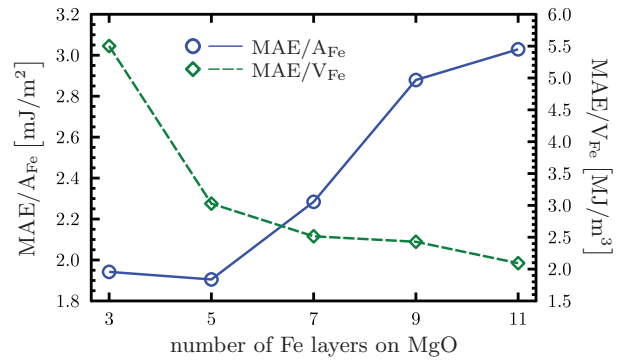
Figure 8. Magnetic anisotropy energy values, MAE/A_{Fe} (blue circles) and MAE/V_{Fe} (green diamonds), as a function of the number of Fe layers n_{Fe}. For a better comparability with other work we note that 1 mJ m^{-2} is equivalent to 1 erg cm^{-2}, and 1 J m^{-3} is equivalent to 10 erg cm^{-3}.

Although this is beyond the scope of the present paper, we have investigated this aspect in another study that will be published elsewhere. Comparing our results to other published work we refer to [27]. In figure 2 in this paper the authors show the MAE depending on the Fe-thickness for a similar system with a substrate (MgO) thickness of 11 monolayers. Considering the odd numbers of iron layers the authors report a linear increase of the MAE when n_{Fe} increases from 5 to 7. The MAE reaches its maximum for $n_{Fe} = 9$ and decreases slightly for $n_{Fe} > 9$. The qualitative behaviour is in good agreement with our findings. Between 5 and 9 Fe layers we also observe an almost linear increase in figure 8 (see MAE/A_{Fe}) and a nonlinear increase for $n_{Fe} > 9$ indicating the aforementioned possible maximum for $n_{Fe} > 11$. Regarding a quantitative comparison we find that for the example of $n_{Fe} = 11$ the relative difference between the values calculated in the present paper (3.0 mJ m^{-2}) and the one obtained in [27] (3.5 mJ m^{-2}) is approx. 14%. Given the difference in the thickness of the substrate (in our study we have a thickness of 5MgO layers whereas [27] use 11MgO) we are confident that this numerical discrepancy is within reasonable tolerance. This is further underpinned by the results obtained in [31] and [16]

where the authors report similar increases in the MAE when increasing the MgO thickness. To compare the value obtained for $n_{Fe} = 3$ in our present paper we use a result from [21]. In this study the authors employ a fully relativistic screened-Korringa–Kohn–Rostoker method based on spin density functional theory (see reference for details). The authors find a value of 1.75 mJ m^{-2} for a MgO|Fe(3ML)|MgO(3ML)|Fe(3ML)|MgO system, whereas we obtain a value of 1.95 mJ m^{-2} (relative discrepancy 11%). Taking into account the different underlying models and methods used, the agreement of the numerical values seems to be reasonable.

4. Conclusions

In the present paper we have studied the geometry, electronic structure and magnetic properties of n_{Fe}Fe|5MgO configurations ($n_{Fe} = 3, 5, 7, 9, 11$) by means of first-principles fully relativistic calculations. The use of metastable geometries is of paramount importance in magnetism, as it will influence important physical quantities such as magnetic moments or magnetic anisotropy. To this end we performed full relaxation of each configuration employing the CG method. Due to the different in-plane lattice constants of Fe and MgO we used the optimized MgO value as initial guess for both. The resulting out-of-plane values changed for each material, i.e. $c_{Fe} \neq c_{MgO}$. This has an important consequence for the anisotropy values that are influenced not only by the number of Fe layer but also by the geometry of the system as explained in section 3.4. The magnetic moments are higher at the interface reducing their values moving inwards to the centre of the bilayer. In general, the magnetic moment in the centre is larger than the bulk value of 2.17 μ_B per atom. Furthermore, the magnetic anisotropy energy increases its absolute value with the Fe thickness, however, the MAE per area seems to reach a plateau with value $\geqslant 3.0$ mJ m^{-2}. The reason for this effect is that only the on-site Fe values close to the interface contribute significantly to the total MAE. Hence, as the Fe subsystem increases in size, the centre of the material resembles the Fe bulk. For sufficiently large iron thicknesses the contribution to the MAE stemming from the centre is negligible and comparable to bulk Fe where it ranges in the order of μeV.

Our results are in agreement with the findings reported in [31] who first showed the importance of Fe–O hybridization in Fe|MgO bilayer systems. However, our detailed analysis of the electronic structure, magnetic moments and charge transport provides important new insight for employing Fe|MgO bilayer systems in future data storage devices. We hope our work further stimulates experimental and theoretical studies aiming at the understanding and development of next generation technologies.

Acknowledgments

References

[1] Faure-Vincent J, Tiusan C, Bellouard C, Popova E, Hehn M, Montaigne F and Schuhl A 2002 *Phys. Rev. Lett.* **89** 107206
[2] Andersson G, Burkert T, Warnicke P, Björck M, Sanyal B, Chacon C, Zlotea C, Nordström L, Nordblad P and Eriksson O 2006 *Phys. Rev. Lett.* **96** 037205
[3] Endo M, Kanai S, Ikeda S, Matsukura F and Ohno H 2010 *Appl. Phys. Lett.* **96** 212503
[4] Nistor L E, Rodmacq B, Auffret S and Dieny B 2009 *Appl. Phys. Lett.* **94** 012512
[5] Katayama T, Yuasa S, Velev J, Zhuravlev M Y, Jaswal S S and Tsymbal E Y 2006 *Appl. Phys. Lett.* **89** 112503
[6] Chiang Y F, Wong J J I, Tan X, Li Y, Pi K, Wang W H, Tom H W K and Kawakami R K 2009 *Phys. Rev.* B **79** 184410
[7] Ikeda S, Miura K, Yamamoto H, Mizunuma K, Gan H D, Endo M, Kanai S, Hayakawa J, Matsukura F and Ohno H 2010 *Nat. Mater.* **9** 721–4
[8] Zhang X G and Butler W H 2004 *Phys. Rev.* B **70** 172407
[9] Turek I, Kudrnovský J and Carva K 2012 *Phys. Rev.* B **86** 174430
[10] Aas C J, Hasnip P J, Cuadrado R, Plotnikova E M, Szunyogh L, Udvardi L and Chantrell R W 2013 *Phys. Rev.* B **88** 174409
[11] Delczeg-Czirjak E K, Edström A, Werwiński M, Rusz J, Skorodumova N V, Vitos L and Eriksson O 2014 *Phys. Rev.* B **89** 144403
[12] Cuadrado R, Klemmer T J and Chantrell R W 2014 *Appl. Phys. Lett.* **105** 152406
[13] Cuadrado R and Chantrell R W 2014 *Phys. Rev.* B **89** 094407
[14] Nakamura K, Ikeura Y, Akiyama T and Ito T 2015 *J. Appl. Phys.* **117** 17C731
[15] Chappert C, Fert A and Van Dau F N 2007 *Nat. Mater.* **6** 813–23
[16] Yamanouchi M, Koizumi R, Ikeda S, Sato H, Mizunuma K, Miura K, Gan H D, Matsukura F and Ohno H 2011 *J. Appl. Phys.* **109** 07C712
[17] Yakata S, Kubota H, Suzuki Y, Yakushiji K, Fukushima A, Yuasa S and Ando K 2009 *J. Appl. Phys.* **105** 07D131
[18] Wang W X, Yang Y, Naganuma H, Ando Y, Yu R C and Han X F 2011 *Appl. Phys. Lett.* **99** 012502
[19] Bonell F *et al* 2012 *Phys. Rev. Lett.* **108** 176602
[20] Andrieu S, Calmels L, Hauet T, Bonell F, Le Fèvre P and Bertran F 2014 *Phys. Rev.* B **90** 214406
[21] Zhang J, Franz C, Czerner M and Heiliger C 2014 *Phys. Rev.* B **90** 184409
[22] Kim G, Sakuraba Y, Oogane M, Ando Y and Miyazaki T 2008 *Appl. Phys. Lett.* **92** 172502
[23] Feng X, Bengone O, Alouani M, Lebègue S, Rungger I and Sanvito S 2009 *Phys. Rev.* B **79** 174414
[24] Yang H X, Chshiev M, Kalitsov A, Schuhl A and Butler W H 2010 *Appl. Phys. Lett.* **96** 262509
[25] Nakamura K, Akiyama T, Ito T, Weinert M and Freeman A J 2010 *Phys. Rev.* B **81** 220409
[26] Lambert C H, Rajanikanth A, Hauet T, Mangin S, Fullerton E E and Andrieu S 2013 *Appl. Phys. Lett.* **102** 122410
[27] Hallal A, Yang H X, Dieny B and Chshiev M 2013 *Phys. Rev.* B **88** 184423
[28] Ringer S, Vieth M, Bär L, Rührig M and Bayreuther G 2014 *Phys. Rev.* B **90** 174401
[29] Mukherjee S *et al* 2015 *Phys. Rev.* B **91** 085311
[30] Neggache A *et al* 2014 *Appl. Phys. Lett.* **104** 252412
[31] Yang H X, Chshiev M, Dieny B, Lee J H, Manchon A and Shin K H 2011 *Phys. Rev.* B **84** 054401

[32] Baumann S *et al* 2015 *Phys. Rev. Lett.* **115** 237202

[33] Niranjan M K, Duan C G, Jaswal S S and Tsymbal E Y 2010 *Appl. Phys. Lett.* **96** 222504

[34] Maruyama T *et al* 2009 *Nat. Nanotechnol.* **4** 158–61

[35] Wang W G, Li M, Hageman S and Chien C L 2012 *Nat. Mater.* **11** 64–8

[36] He K H, Chen J S and Feng Y P 2011 *Appl. Phys. Lett.* **99** 072503

[37] Duluard A, Bellouard C, Lu Y, Hehn M, Lacour D, Montaigne F, Lengaigne G, Andrieu S, Bonell F and Tiusan C 2015 *Phys. Rev.* B **91** 174403

[38] Cuadrado R and Cerdá J I 2012 *J. Phys.: Condens. Matter* **24** 086005

[39] Cerdá J, Van Hove M A, Sautet P and Salmeron M 1997 *Phys. Rev.* B **56** 15885–99

[40] Soler J M, Artacho E, Gale J D, García A, Junquera J, Ordejón P and Sánchez-Portal D 2002 *J. Phys.: Condens. Matter* **14** 2745

[41] Perdew J P, Burke K and Ernzerhof M 1996 *Phys. Rev. Lett.* **77** 3865–8

[42] Mulliken R S 1955 *J. Chem. Phys.* **23** 1833–40

[43] Chepulskyy R, Apalkov D, Khvalkovskiy A, Butler W, Ahn H and Krounbi M 2013 Separate contributions into perpendicular magnetic anisotropy of Fe–MgO interface from first-principles *12th Joint MMM/Intermag Conf. (Chicago, IL, USA, 14–18 January 2013)*

[44] Apalkov D, Chepulskyy R, Khvalkovskiy A, Nikitin V, Watts S, Visscher P, Butler W, Ahn H and Krounbi M 2013 Perpendicular STT-MRAM: origins of anisotropy, scalability and challenges *Int. French-US Workshop 'Toward Low Power Spintronic Devices' (La Jolla, CA, USA, 8–12 July 2013)*